Molecular Psychiatry (2013) 18, 382 – 393

www.nature.com/mp

ORIGINAL ARTICLE

Co-activation of VTA DA and GABA neurons mediates nicotine reinforcement

S Tolu[1,2,11], R Eddine[3,11], F Marti[3,11], V David[4], M Graupner[5], S Pons[1,2], M Baudonnat[4], M Husson[4], M Besson[1,2], C Reperant[6], J Zemdegs[6], C Pagès[7], YAH Hay[8], B Lambolez[8], J Caboche[7], B Gutkin[9], AM Gardier[6], J-P Changeux[2,10], P Faure[3,11] and U Maskos[1,2,11]

Smoking is the most important preventable cause of mortality and morbidity worldwide. This nicotine addiction is mediated through the nicotinic acetylcholine receptor (nAChR), expressed on most neurons, and also many other organs in the body. Even within the ventral tegmental area (VTA), the key brain area responsible for the reinforcing properties of all drugs of abuse, nicotine acts on several different cell types and afferents. Identifying the precise action of nicotine on this microcircuit, *in vivo*, is important to understand reinforcement, and finally to develop efficient smoking cessation treatments. We used a novel lentiviral system to re-express exclusively high-affinity nAChRs on either dopaminergic (DAergic) or γ-aminobutyric acid-releasing (GABAergic) neurons, or both, in the VTA. Using *in vivo* electrophysiology, we show that, contrary to widely accepted models, the *activation* of GABA neurons in the VTA plays a crucial role in the control of nicotine-elicited DAergic activity. Our results demonstrate that both positive and negative motivational values are transmitted through the dopamine (DA) neuron, but that the *concerted* activity of DA and GABA systems is necessary for the reinforcing actions of nicotine through burst firing of DA neurons. This work identifies the GABAergic interneuron as a potential target for smoking cessation drug development.

Molecular Psychiatry (2013) **18,** 382–393; doi:10.1038/mp.2012.83; published online 3 July 2012

Keywords: dopamine; GABAergic interneuron; lentiviral vector; nicotine addiction; nicotinic acetylcholine receptor

INTRODUCTION

Tobacco abuse is the worldwide leading cause of preventable morbidity and mortality. According to the World Health Organization, more than five million smokers die every year from the consequences.[1] Dissecting the underlying neurobiological mechanisms of this disorder has recently made important progress with the use of genetically modified mice,[2] but they remain far from being understood in detail. The identification of novel drug targets for the design of smoking cessation medication is becoming a priority in pharmacological research.[3] Nicotine, the principal, if not sole, addictive component of tobacco smoke,[4] exerts its reinforcing effects through its action on nicotinic acetylcholine receptors (nAChRs), a heterogeneous family of pentameric, ligand-gated ion channels.[5] nAChRs situated in the mesolimbic reward system mediate nicotine-induced dopamine (DA) release in the nucleus accumbens (NAc) from midbrain dopaminergic (DAergic) neurons located in the ventral tegmental area (VTA).[6] Among the different nAChRs expressed in this region, β2-containing nAChRs (β2*-nAChRs) have been shown to play a crucial role in the positive rewarding properties of nicotine, as they are the essential partner to form high-affinity receptors.[7] β2*-nAChRs are expressed on both DAergic and γ-aminobutyric acid-releasing (GABAergic) interneurons present in the VTA,[8] and nicotine modulates the activity of both neuronal populations.[9] Pharmacological studies have addressed the complex and often opposing influences of the DA- and GABA-dependent neural systems,[10] but none of them has yet elucidated the nature of their interaction, that is, whether they cooperate to produce the rewarding effect,[9,11,12] or mediate, respectively, the acute rewarding and aversive psychological effects of nicotine.[10]

The complexity of nicotine's action to result in enhanced DA release has been reviewed recently.[13,14] Several independent mechanisms have been identified, or postulated. These are enhanced excitation of the DA cells,[15] or their disinhibition, or modification of presynaptic terminals onto the soma of DA neurons. Previous *in vitro* studies proposed that the desensitization of β2*-nAChRs on GABA interneurons following nicotine exposure, resulting in decreased GABAergic neuron activity, produces a disinhibition of DA neurons, and hence increased presynaptic excitation.[9,11,16] We have here comprehensively addressed the respective role of β2*-nAChRs expressed on DA or GABAergic VTA neurons in their response to nicotine, and the behavioral consequences. The work presented is arranged according to the following outline: using *in vivo* electrophysiology of single neurons in the VTA, we found surprisingly that putative GABAergic neurons do not desensitize following repeated nicotine injections as postulated by current models. We then set out to understand the physiological basis of their role in DA neuron

[1]Département de Neuroscience, Institut Pasteur, Unité Neurobiologie intégrative des systèmes cholinergiques, Paris, France; [2]CNRS, URA2182, Paris, France; [3]Université P. et M. Curie, CNRS UMR 7102, Neurobiologie des Processus Adaptatifs, Equipe Neurophysiologie et comportement, Paris, France; [4]Université de Bordeaux, Institut de Neurosciences Cognitives et Intégratives d'Aquitaine, Talence, France; [5]Center for Neural Science, New York University, New York, NY, USA; [6]EA3544 Pharmacologie des troubles anxio-dépressifs et Neurogenèse, Univ Paris-Sud, Fac Pharmacie, Châtenay-Malabry, France; [7]Université P. et M. Curie, INSERM UMRS 952, CNRS UMR 7224, Physiopathologie des Maladies du Système Nerveux Central, Equipe Signalisation Intracellulaire et Neuroadaptations, Paris, France; [8]Université P. et M. Curie, CNRS UMR 7102, Neurobiologie des Processus Adaptatifs, Equipe Réseau cortical et couplage neurovasculaire, Paris, France; [9]Group for Neural Theory, LNC INSERM U960, DEC ENS, Paris, France and [10]Collège de France, Paris, France. Correspondence: U Maskos or P Faure, Département de Neuroscience, Institut Pasteur, Unité Neurobiologie intégrative des systèmes cholinergiques, Institut Pasteur, 25 rue du Dr Roux, Cedex 15, Paris 75724, France.
E-mail: umaskos@pasteur.fr or philippe.faure@snv.jussieu.fr
[11]These authors contributed equally to this work.
Received 5 December 2011; revised 2 May 2012; accepted 7 May 2012; published online 3 July 2012

activity. This was achieved by the selective expression of high-affinity nicotinic receptors on either DA or GABAergic interneurons, or both, and the correlation of DA firing patterns with intra-VTA self-administration behavior. We conclude that GABA-dependent burst firing of DA neurons is a crucial element in the reinforcing effect of nicotine.

MATERIALS AND METHODS

Viral production and analysis of transduced VTA cells

Viral production. Viral particles were generated by co-transfection of HEK-293T cells by the vector plasmid, a packaging plasmid and an envelope plasmid using Lipofectamine Plus (Invitrogen, Carlsbad, CA, USA) according to the manufacturer's instructions. At 2 days after transfection, viral particles were harvested in the supernatant, treated with DNaseI and $MgCl_2$, filtered through 0.45 μm pores, concentrated by ultracentrifugation and resuspended in a small volume of phosphate-buffered saline (PBS). Viral stocks were stored in small aliquots at −80 °C before use. Viral titers were estimated by quantification of the p24 capsid protein using HIV-1 p24 antigen immunoassay (ZeptoMetrix Corporation, Buffalo, NY, USA) according to the manufacturer's instructions. Lentivectors were diluted in PBS before stereotaxic injection to achieve a dose corresponding to 230 ng of p24 protein in 2 μl.

Stereotaxic procedure. Mice aged 6–12 weeks were anesthetized using ketamine/xylazine in PBS. A mouse was introduced into a stereotaxic frame adapted for use with mice. Lentivectors (enhanced green fluorescent protein (eGFP)-expressing vector: 2 μl at 50 ng p24 protein per μl; β2-expressing vector: 2 μl at 115 ng p24 protein per μl) were injected bilaterally at: antero-posterior −3.4 mm, lateral ± 0.5 mm from Bregma and −4.4 mm from the surface. All procedures were carried out in accordance with European Commission directives 219/1990 and 220/1990, and approved by Animalerie centrale and Médecine du travail, Institut Pasteur. The authors carrying out surgery hold an Animal Surgery Authorization from the French Ministry of Agriculture.

Analysis of transduced VTA cells

Immunostaining. To analyze eGFP and mCherry transduction on DAergic and GABAergic neurons, sections from vectorized DAT-Cre and GAD67-Cre mice were stained for tyrosine hydroxylase (TH) antibody. Fluorescence immunohistochemistry was performed as follows: free-floating VTA brain sections were incubated 1 h at 4 °C in a fixative solution of PBS containing 10% normal goat serum (Sigma, Lyon, France) and 0.2% Triton X-100, and then overnight at 4 °C in PBS containing a mouse anti-TH (Sigma) at 1:200 dilution, 2% normal goat serum and 0.2% Triton X-100. The next day, sections were rinsed with PBS and then incubated 3 h at room temperature with secondary antibody (Cy5-coniugated anti-mouse, Jackson Immunoresearch, London, UK) at 1:200 dilution in a solution of 2% normal goat serum in PBS. After three rinses in PBS, slices were wet-mounted using Mowiol 4-88 (Calbiochem Corporation, La Jolla, CA, USA).

Cell counting by image analysis. Anti-TH-immunostained sections from DAT-Cre mice were imaged at × 25, × 40 and × 63 with a Zeiss LSM510 confocal laser scanning microscope (Carl Zeiss, Oberkochen, Germany). A quantitative analysis of transduced neurons was performed automatically with the software identifying spot positions using a statistical analysis of the multiscale decomposition of the image. The program (QUIA; http://www.bioimageanalysis.org) detects nuclei (Cre-positive cells) by first filtering the image with an undecimated wavelet at different scales and then thresholding it with a statistical procedure,[17,18] which takes into account the noise level. To perform colocalization, we computed for each pixel of each detection the number of corresponding pixels in the green channel (eGFP-positive cells), considering a fixed threshold. The detection is labeled as colocalized if the number of green pixels reaches 50% of the area of the nuclei. For phosphorylated-extracellular signal-regulated kinase (P-ERK) immunostaining, quantifications were performed using the image analyzer software (Image-Pro Plus; Media Cybernetics, Silver Spring, MD, USA), taking into account the cells with nuclear immunofluorescence above the background.

Determination of the efficiency of DA cell transduction

The percentage of transduced TH-positive neurons in vectorized DAT-Cre mice was quantified on one of every three sections for each mouse. This results in 73 ± 12% of DA neurons being transduced.

Epibatidine binding studies

The $\beta^{-/-}$, $\beta2^{-/-}$ × DAT-Cre and $\beta2^{-/-}$ × GAD-Cre mice aged 12–13 weeks were injected bilaterally in the VTA. After 4 weeks of viral expression, brains were dissected, frozen in dry ice and stored at −80 °C until use. Coronal sections, 20-μm thick, were cut at −20 °C and thaw mounted on Menzel Glasser SuperFrost Plus microscope slides. Slides were incubated at room temperature with 220 pM ^{125}I-epibatidine (NEN Perkin-Elmer, Boston, MA, USA; specific activity 2200 Ci/mmol) in 50 mM Tris (pH 7.4) for 1 h. After incubation, sections were rinsed twice 5 min in the same buffer and briefly in distilled water. Nonspecific binding was not distinguishable from background. Sections were exposed for 36 h to Kodak Biomax films. As reported previously,[19] high-affinity ^{125}I-epibatidine binding sites were absent from the brain of β2 knockout (KO) mice, with the exception of structures of the habenulo-peduncular system. The quantification of lentiviral restoration of functional β2*-nAChRs in the VTA was carried out by ImageJ (National Institutes of Health, Bethesda, MD, USA) on eight coronal sections for each brain. To obtain the mean value of the optical density, the same ROI was reported on every section of each brain.

In vivo electrophysiological recording of VTA DAergic and GABAergic neurons

Single unit extracellular recordings were performed in wild-type (WT), KO and VEC (vectorized) mice as detailed in the Supplementary Information. Animals were anesthetized with chloral hydrate (400 mg/kg, intraperitoneally). Spontaneously active DA and GABA neurons were identified on the basis of previously established electrophysiological criteria (see Supplementary Material and Mameli-Engvall *et al*.[15]). Intravenous injection of 0.5 mM nicotine tartrate into the saphenous vein (30 μg/kg free base in a final volume of 10 μl) was performed as described. Firing frequency was quantified over 30 s periods, expressed as a percentage of average basal firing, and means were calculated within each group.

In vitro electrophysiological recording of VTA DAergic and GABAergic neurons

Slice recordings were performed in WT, KO and VEC mice as detailed in the Supplementary Information.

In vivo microdialysis

In vivo microdialysis was carried out as described in the Supplementary Information, with a probe placed unilaterally in the shell of the NAc, coordinates from Bregma (in mm): anterior 1.34, lateral 0.7, ventral −5.4. Probe placement was verified histologically.

Intracranial self-administration procedure

Intracranial self-administration (ICSA) behavior was investigated using a procedure previously described for morphine[20,21] and cocaine,[22,23] and then adapted to nicotine.[19,24] This model is based on choice behavior in a Y-maze discrimination task between a nicotine-reinforced arm and a neutral arm. Discrimination tasks relying on choice behavior provide a more accurate assessment of reward than rate-dependent paradigms.[25] This task is particularly well adapted to detect reward-related deficits in mutant mice.[24,26,27] ICSA allows excellent temporal and spatial, region-specific delivery of nicotine for targeting specifically brain structures such as the VTA.[24,28] The present experiments were conducted in a gray Plexiglas Y-maze, see Figure 4a. Its arms were separated by an angle of 90°. The stem and the arms were 31 cm long and 12 cm high. The starting box ($14 \times 8\,cm^2$) is separated from the stem by a sliding door. Each arm is

composed of a sliding door at its entrance and a photoelectric cell 6 cm from its end. Mice are implanted unilaterally into the posterior VTA, using the coordinates of lentiviral injections. Before each experimental session, a stainless-steel injection cannula (outer diameter 0.229 mm, inner diameter 0.127 mm; Figure 4a) is inserted into the VTA and held in a fixed position by means of a small connector. The tip of the injection cannula projects beyond the guide cannula by 1.5 mm (Figure 4a). It is connected by flexible polyethylene tubing to the microinjection system, which houses a 5-μl Hamilton syringe containing a solution of nicotine in the artificial cerebrospinal fluid (Microperfusion Fluid; Phymep, Paris, France), the pH of which being adjusted to neutrality with NaOH 0.1 N. Mice were tested for nine consecutive days, with each daily session composed of 10 successive trials. The first session consisted in a 10-min free exploration of the Y-maze. During a second session, mice were habituated to be connected to the self-injection system, but no injection was available. In subsequent sessions, interruption of photocell beams by entering the reinforced arm of the Y-maze triggered an intra-VTA injection of nicotine that lasted 4 s (100 ng nicotine tartrate in 50 nl of artificial cerebrospinal fluid, resulting in a nicotine concentration of 4 mM as referred to the base). As photobeams are located only 6 cm from the end of each arm, mice had to enter completely into an arm to end a trial. Therefore, partial entrance into the arm did not count as a choice. Entering completely the non-reinforced arm produces no injection, and entering either arm terminated the trial. The animal's movements are detected using an optical system and transmitted to a computer, which rotated in turn the injector in the same direction, thus avoiding twisting. The number of times mice trigger a self-injection within the nicotine-reinforced arm (the number of self-administrations) and the time between the opening of the starting box door and triggering of self-injections (self-injection latency) were recorded by a computer running a program specifically developed for ICSA (YAA; Imetronic, Pessac, France). The mean of one daily session provided one graph plot. Both WT and mutant mice exhibited a similar number of intra-VTA injections of vehicle (artificial cerebrospinal fluid, data not shown) that was not different from chance level (50%). All groups were constituted of at least $n = 7$ and up to $n = 10$ subjects per group. Following thionin-stained histological control of stereotaxic implantation, only mice with a self-injection cannula located within the VTA were included in the statistical analysis. For the ICSA, all data were analyzed by repeated measures analysis of variance using StatView 5.0 (Abacus Concepts, Piscataway, NJ, USA), followed by *post-hoc* Fisher's test for which the level of statistical significance was set at $P < 0.05$.

RESULTS

In vivo electrophysiology of the nicotine response in the VTA

We wanted to obtain a comprehensive understanding of nicotine responses in the microcircuits of the VTA. As most previous studies were carried out in slice preparations, we decided to address the nicotinic-cholinergic regulation of the VTA using *in vivo* electrophysiology.[15] There, all afferents to the VTA are preserved, and in particular the cholinergic input from the tegmentum, a key player in VTA physiology[29,30] (see Figure 1). Intravenous administration of nicotine (30 μg/kg) in naive animals resulted in a rapid and pronounced increase in the firing rate of DA cells (Figure 2a), and also of putative GABAergic interneurons (Figure 2b). This latter result is incompatible with a rapid, desensitization-dependent decrease in GABA activity postulated by the disinhibition hypothesis. We then performed paired injections of nicotine at intervals of 5 or 15 min. If disinhibition were the main mechanism underlying the DA cell response, subsequent nicotine injections would further enhance receptor desensitization in GABA neurons, resulting in an increase in the consecutive peak response of DA cells to nicotine. At a 15-min interval, when no accumulation of nicotine in blood and brain was possible due to nicotine pharmacokinetics,[31] we observed no change in the amplitude of the DA response to nicotine (Figure 2c). However, at the interval of 5 min, allowing accumulation of nicotine upon injections, DA

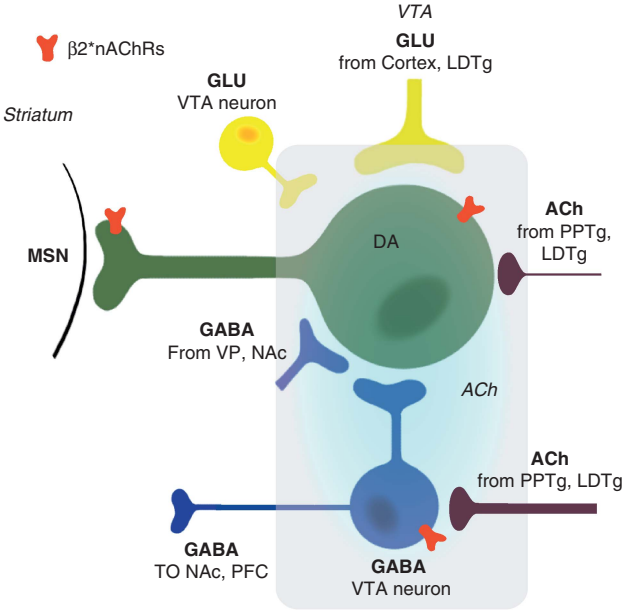

Figure 1. A schematic representation of the ventral tegmental area (VTA) and afferents. The focus of the work is on the shaded area of the VTA. The dopaminergic (DAergic) output neuron (green) contains high-affinity β2-containing nicotinic acetylcholine receptors (nAChRs) (red). It is locally inhibited by γ-aminobutyric acid-releasing (GABAergic) interneurons that also contain high-affinity β2*-nAChRs. Additional GABAergic projections arrive from the ventral pallidum (VP), and glutamatergic projections from the cortex, the tegmental LDTg (laterodorsal tegmental nucleus, in yellow) and locally from recently identified interneurons. The important feature of cholinergic control in the VTA is the ACh release from afferents originating in the LDTg/PPTg pontine tegmental nuclei.[29,30] Dopamine (DA) is released in the striatum onto medium spiny neurons (MSNs) in the nucleus accumbens (NAc), which show biochemical alterations after stimulation (see Figure 5).

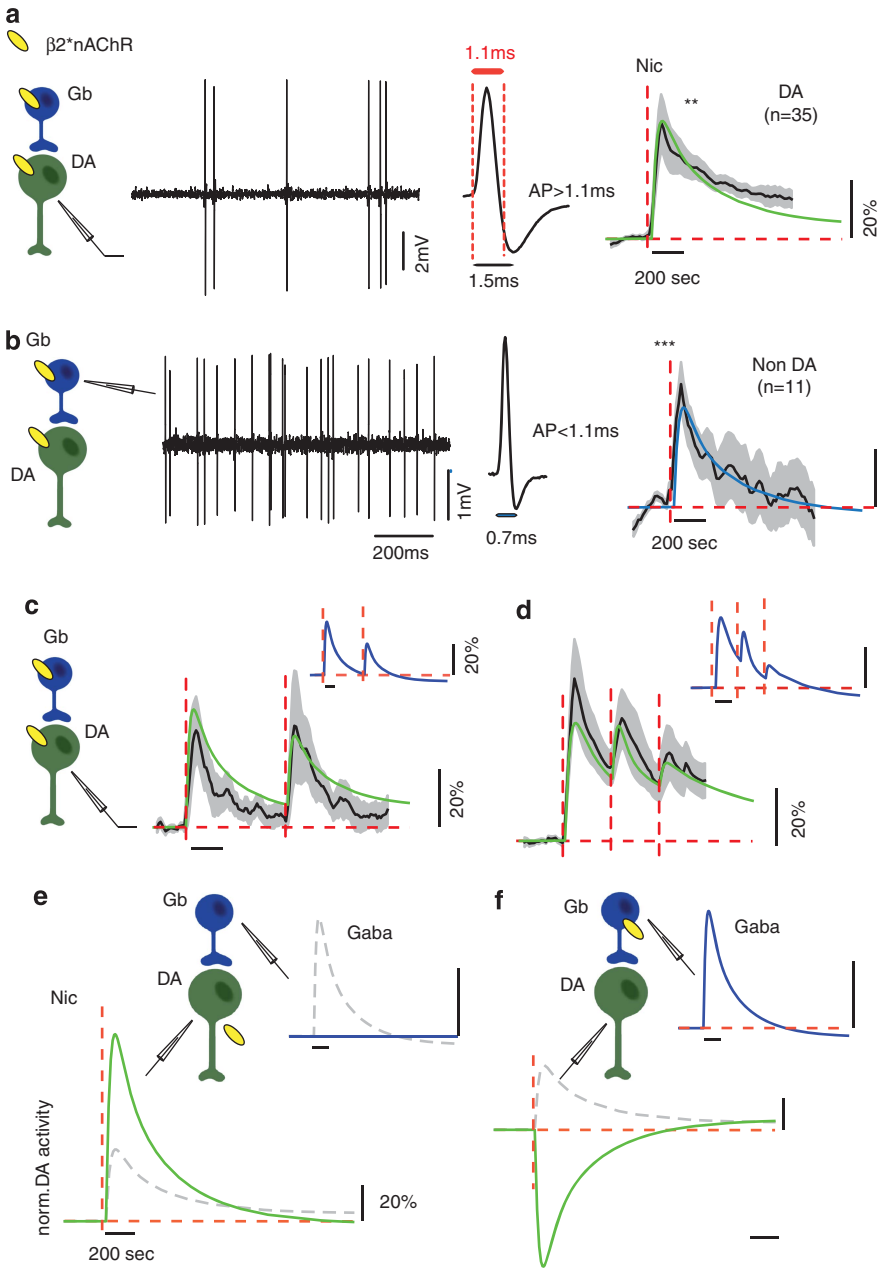

Figure 2. *In vivo* response of ventral tegmental area (VTA) neurons to nicotine and modeling. The sketches to the left of all panels represent the dopamine (DA)/γ-aminobutyric acid (GABA) microcircuit. The dopaminergic (DAergic) neuron is in green (DA) and the γ-aminobutyric acid-releasing (GABAergic) interneuron in blue (Gb). The β2*-nicotinic acetylcholine receptors (nAChRs) in yellow indicate their differential expression between the two cell types, and the electrode marks the cell from which recordings were obtained. The traces obtained with *in vivo* electrophysiological recordings are in black and the standard error painted in gray. Green traces are from the model fitted to the experimental values for DA recordings and the blue trace corresponds to GABA cells. The time points of nicotine (Nic) injections are marked by red vertical dashed lines. (**a**) DA neuron identification and response to nicotine. (Left) Example of raw traces of DA cells (1 among $n = 43$, mean firing rate = 3.31 ± 0.27). (Middle) Example of action potential (AP) waveform of a VTA DAergic neuron. (Right) Nicotine-elicited modifications of firing frequency (mean ± s.e.m.) of VTA DAergic neurons (black, $n = 43$, mean of basal firing rate 3.31 ± 0.27 Hz, mean of the maximal variation + 54.33 ± 12.036%, $P = 1.55 \times 10^{-7}$, Wilcoxon's signed-rank test). Green, model DA activity response to nicotine. (**b**) GABA neuron identification and response to nicotine. (Left) Example of raw traces of GABA neurons (1 among $n = 11$, mean firing rate = 20.06 ± 3.74). (Middle) Example of non-filtered AP waveform of a VTA non-DAergic neuron. (Right) Nicotine-elicited modifications of firing frequency (mean ± s.e.m.) of putative GABAergic neurons ($n = 11$, mean of basal firing rate 20.06 ± 3.74 Hz, mean of the maximal variation + 49.32 ± 6.39%, $P = 0.0009$, Wilcoxon's signed-rank test). Blue, model GABA neuron activity response to nicotine. (**c**) DA neuron response to two repeated nicotine injections with an interval of 15 min ($n = 7$, mean of basal firing rate 3.67 ± 0.8 Hz). Inset shows corresponding GABA responses, in blue. (**d**) DA neuron response to three repeated nicotine injections at 5-min intervals ($n = 11$, mean of basal firing rate 3.41 ± 0.38 Hz). Inset shows corresponding GABA responses. Note that the model has been fitted to all four experimental recordings from panels a to d simultaneously. (**e**) Predicted DA neuron response to a single nicotine injection with β2*-nAChRs on DA neurons only, see sketch to the left. (**f**) Predicted DA neuron response to a single nicotine injection with β2*-nAChRs on GABA neurons only, see sketch to the left. All horizontal scale bars are 200 s and vertical scale bars show 20% relative changes in firing rate. Dashed curves show the control responses (that is, ß2 on both DA and GABA neurons) for comparison.

neurons exhibited a decrease in the amplitude of nicotine response (Figure 2d). Therefore, *in vivo*, the immediate firing rate increase of DAergic cells in response to an acute injection of nicotine entails DA excitation, and a competition with inhibition, rather than desensitization of nAChRs on GABAergic interneurons.

Modeling the *in vivo* response to nicotine

To corroborate the proposed direct excitation mechanism of nicotine action, we used a minimal model of the VTA microcircuit to account quantitatively for the recorded responses of DA and GABA neurons, a model modified from Graupner and Gutkin.[32,33] The model reflects the cholinergic (ACh) afferents to the DA and GABA cells in the VTA, local inhibition of DA cells by GABA neurons as well as the pharmacology of the nAChRs (Figure 1). In this minimal model, we chose to leave aside a potential contribution from local glutamatergic neurons as described very recently, as no data exist as to their expression of nicotinic receptors.[34] Nicotine-evoked changes are thus exclusively mediated by β2*-nAChRs expressed somatically on both DA and GABA neurons. This is in line with experiments and modeling studies suggesting that the ß2-containing subtype plays the dominant role in nicotinic modulation of DA signaling.[7,15,32,35]

The model, see Supplementary Information, fitted to the recordings of DA and GABA firing rate responses (green and blue traces in Figure 2), respectively, shows that nicotine drives both β2*-nAChR activation and desensitization. The early response to nicotine in DA and GABA neurons, for example, to a single nicotine injection, is dominated by direct receptor activation that boosts the firing rates in both neuron types (Figures 2a and b). Subsequent nicotine injections further recruit receptor desensitization giving rise to an accommodation in the peak response of DA cells to nicotine (Figures 2c and d). This accommodation is stronger for shorter inter-injection intervals (compare Figure 2c for 15-min intervals and Figure 2d for 5 min). In addition, in our model nicotine-dependent receptor desensitization in GABA neurons decreases their firing rate below baseline after nicotine clearance, thereby producing a prolonged elevated DA response in the model (see Figures 2c and d).

Experimental and model data suggest that receptor desensitization does not govern the immediate DA response and confirms the predominant role of early excitation due to acute nicotine. The model results furthermore suggest that long-lasting disinhibition might give rise to a secondary delayed and prolonged elevated DA activity after nicotine clearance (Figures 2c and d). Finally, these results also suggest that both DA and GABA pathways are activated by nicotine. Dissociating the consequences of the activation of the two pathways by acute nicotine on firing of identified DA cells would confirm the respective role of β2*-nAChRs on DA and GABA neurons. A simulation of two variants of the model, that is, where we set β2*-nAChRs to be expressed only on DA neurons, or only on the GABA neurons, illustrates the potential benefit of this experiment. The first model gives rise to a rapid DA activity boost through direct nicotine-evoked excitation of DA neurons alone (Figure 2e**)**. The second yields only a nicotine-evoked immediate inhibition of the DA firing rate (Figure 2f). This predicts that a differential expression of β2*-nAChRs on the DA or on the GABA neuron would favor excitation versus inhibition of the DA firing rates.

A novel system for the cell-type-specific expression of nicotinic receptors

To test these respective *in vivo* roles of the DAergic and GABAergic neurons in the microcircuits involved in nicotine reinforcement, we used a Cre recombinase-activated lentiviral expression vector[18] (Figure 3a) to drive specific β2*-nAChR re-expression in DA or GABAergic neurons of the VTA. We created two new mouse lines expressing Cre recombinase only in DAergic neurons ($\beta2^{-/-} \times$ DAT-Cre mice),[36] or only in GABAergic neurons ($\beta2^{-/-} \times$ GAD67-Cre mice).[18,37] [^{125}I]Epibatidine autoradiography on coronal brain slices demonstrated the recovery of high-affinity receptors at the injection site in the VTA and in axon terminals in the NAc (Figure 3b) for vectorized $\beta2^{-/-} \times$ DAT-Cre mice (referred to as $\beta2^{DA-VEC}$), but only in the VTA for $\beta2^{-/-} \times$ GAD67-Cre mice ($\beta2^{GABA-VEC}$) injected with the floxed lentivirus. Sections of these mice labeled with epibatidine were quantified, and as shown in Supplementary Figure S2, restoration of between 70 and 85% of

Figure 3. Generation and analysis of $\beta2^{DA-VEC}$, $\beta2^{GABA-VEC}$ and $\beta2^{DA+GABA-VEC}$ mice. (**a**) Schematic representation of the lentiviral vectors used in this study, conditionally expressing the β2 subunit or eGFP. Cre recombinase recognizes the two loxP sites and removes the mCherry-Stop DNA sequence, activating β2 subunit expression. Restriction enzymes used in the DNA construct are indicated above the vector. (**b**) [^{125}I]Epibatidine autoradiography on coronal brain slices of axon terminals in the nucleus accumbens (NAc) (top) and in the ventral tegmental area (VTA) (bottom), in $\beta2^{DA-VEC}$ mice (left) and $\beta2^{GABA-VEC}$ (right) mice. Arrowheads point to axonal label in the NAc and arrows to somatic label in the VTA (circled). (**c**) mCherry and eGFP expression in VTA sections of DAT-Cre and GAD67-Cre mice. eGFP expression (green) is restricted to tyrosine hydroxylase (TH)-positive neurons (blue) of DAT-Cre mice (left) and to TH-negative neurons of GAD67-Cre mice (right). mCherry expression (red) was only found in TH-negative neurons of DAT-Cre mice (left), and only in TH-positive neurons of GAD67-Cre mice (right). Scale bar, 20 μm. (**d**) Summary of the size of DAergic neuron populations used in this study and proportion of labeled cells. (Top, left) Example of labeling showing colocalization of neurobiotin (blue) and TH (red), allowing identification of the recorded neuron. (Top, right) Raster plot of raw traces from electrophysiological recordings; 50 s before and 50 s after nicotine injection (Nic) are shown. Colors correspond to $\beta2^{DA-VEC}$ (green), $\beta2^{-/-}$ (red) and $\beta2^{GABA-VEC}$ (blue). Scale bar, 10 s. (Bottom) Table summarizing the pool of DA neurons recorded and labeled in this study. (**e**) Nicotine-elicited modifications of firing frequency (mean ± s.e.m.) in VTA DAergic neurons. Sketches to the left indicate the differential expression of the β2*-nicotinic acetylcholine receptors (nAChRs) (yellow) in DA (green) or GABA neurons (blue), and the recorded neuron (electrode, always the DA neuron). Vertical dashed line indicates the nicotine injection (blue). Horizontal dashed line indicates the baseline level (red). (Top) DAergic neurons in $\beta2^{DA-VEC}$ mice (green, $n = 20$, mean of basal firing rate 2.62 ± 0.24 Hz, mean of the maximal variation + 22.54 ± 7.03%, $P = 0.00032$, Wilcoxon's signed-rank test). (Second row) DAergic neurons in $\beta2^{-/-}$ mice (red, $n = 27$, mean of basal firing rate 2.28 ± 0.17 Hz, mean of the maximal variation + 2.62 ± 0.24%, $P = 0.7$, Wilcoxon's signed-rank test). (Third row) DAergic neurons in $\beta2^{GABA-VEC}$ mice (blue, $n = 30$, mean of basal firing rate 3.48 ± 0.33 Hz, mean of the maximal variation −22 ± 3.7%, $P = 6 \times 10^{-8}$, Wilcoxon's signed-rank test). (Bottom) DAergic neurons in $\beta2^{DA+GABA-VEC}$ mice (purple, $n = 13$, mean of basal firing rate 2.29 ± 0.43 Hz, mean of maximal variation + 53.16 ± 25.81%, $P = 0.00012$, paired Wilcoxon's test). Group comparison: wild-type (WT) vs $ß2^{-/-}$, $P = 6 \times 10^{-6}$; WT vs $\beta2^{GABA-VEC}$, $P = 1.6 \times 10^{-6}$; $ß2^{-/-}$ vs $\beta2^{DA-VEC}$, $P = 0.006$; $ß2^{-/-}$ vs $\beta2^{GABA-VEC}$, $P = 1.56 \times 10^{-6}$; $\beta2^{-/-}$ vs $\beta2^{DA+GABA-VEC}$, $P = 0.00067$ (Wilcoxon's signed-rank test with a sequential Bonferroni correction). WT was first compared to $ß2^{-/-}$. If significant, a series of six comparisons were then performed (WT or ß2−/− vs $\beta2^{DA-VEC}$, $\beta2^{GABA-VEC}$ or $\beta2^{DA+GABA-VEC}$), only significant comparisons are indicated (see Supplementary Material). β2, mouse wild-type β2 nicotinic acetylcholine receptor subunit cDNA; cPPT, central polypurine tract; CTS, central termination sequence; DA, dopamine; ΔU3, 400bp deletion in 3′-LTR; eGFP, enhanced green fluorescent protein cDNA; GABA, γ-aminobutyric acid; loxP, recognition sites for Cre recombinase; LTR, long terminal repeats; mCherry, monomeric red Cherry fluorescent protein coding sequence; PDGF-β, platelet-derived growth factor β chain promoter; 3′-PPT, 3′-polypurine tract; RNA pack, genomic RNA packaging signal; RRE, rev response element; Stop, multiple STOP codons; VEC, vector.

high-affinity binding sites compared to WT mice were obtained. We injected mice with a GFP-expressing lentivector (Figure 3a)[18] to confirm that transgene expression was completely restricted only to DAergic cells of DAT-Cre mice, and to GABAergic cells of GAD67-Cre mice (Figure 3c), and to quantify the efficiency of the re-expression. We found that 75% of DA neurons re-express the gene with this approach, see Materials and methods. This correlates well with the restoration observed in the binding studies. We also established slice electrophysiology of vectorized mice, see Supplementary Figure S3. We were thus able to demonstrate in an independent set of experiments that vectorization of either the DA or GABA neurons fully restores responsiveness of high-affinity nAChRs.

We then compared nicotine-evoked modification of firing pattern in DAergic neurons of WT mice with those of $\beta2^{-/-}$ (see Supplementary Material for $\beta2^{-/-}$ group definition), $\beta2^{DA-VEC}$ and $\beta2^{GABA-VEC}$ mice (Figures 3d and e). Selective re-expression of the β2 subunit in DAergic neurons only resulted in an increased firing frequency after systemic nicotine injection, whereas $\beta2^{GABA-VEC}$ mice exhibited a decrease (Figure 3e). The duration of the DA cell inhibition in $\beta2^{GABA-VEC}$ tallies well with the duration of GABAergic excitation observed in WT animals (Figure 2b). As with the WT mice (Figures 2c and d), repeated nicotine injections were carried out as shown in Supplementary Figure S4. Similar to WT mice, $\beta2^{DA-VEC}$ exhibited a decrease in the peak response of DA neurons to consecutive injections of nicotine (Supplementary Figure S4b). This is in accordance with model data suggesting that successive nicotine injections further recruit receptor desensitization and give rise to an accommodation in the peak response of DA cells to nicotine. Results suggesting a similar phenomenon were obtained in $\beta2^{GABA-VEC}$ mice (Supplementary Figure S4c). Taken together, these data indicate that ß2*-nAChRs are desensitized by nicotine at the level of both the DA and GABA neurons. However, in WT mice, the net effect of this desensitization, at a timescale on the order of minutes, results in a reduction of the peak response of DA cells, and *not* in a strong disinhibition.

These experiments dissociate the competitive effect of direct nicotine excitation revealed in $\beta2^{DA-VEC}$ and the indirect inhibition through GABAergic nAChR excitation. We had previously shown that the nicotine-elicited increase in the tonic activity of DA cells is

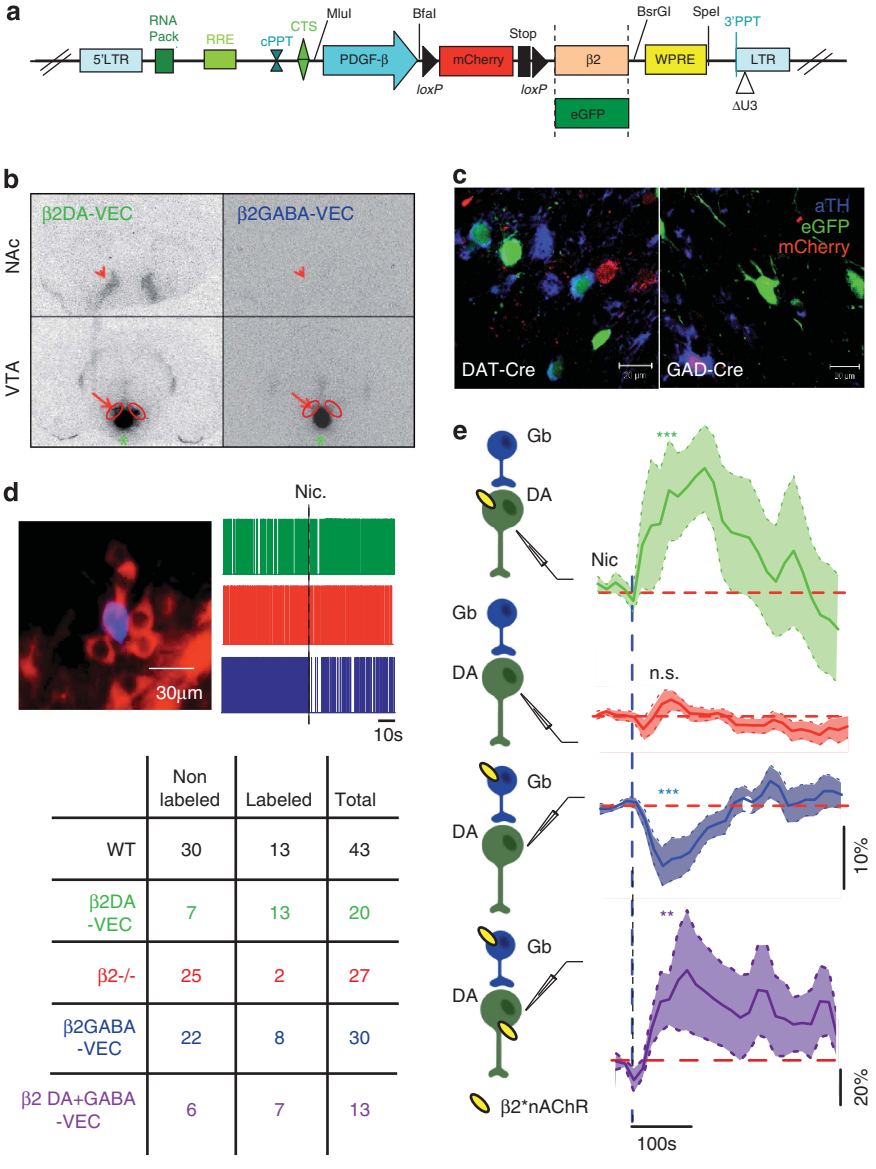

	Non labeled	Labeled	Total
WT	30	13	43
β2DA -VEC	7	13	20
β2-/-	25	2	27
β2GABA -VEC	22	8	30
β2 DA+GABA -VEC	6	7	13

abolished in $\beta2^{-/-}$ mice, and is restored when the β2 subunit is re-expressed in all neurons of the VTA.[15,27] To exclude any possible contribution from other cell types in the VTA, for example, recently described glutamatergic interneurons (see Figure 1), we created a third mouse line crossing the DAT-Cre and GAD67-Cre lines together onto a $\beta2^{-/-}$ background. Injecting theses double transgenic lines with the floxed β2-expressing lentivirus, referred to as $\beta2^{DA+GABA-VEC}$ mice, leads to the targeted expression of the β2 subunit on *both* DA and GABA neurons, but not any other cell type. Injecting nicotine intravenously into these mice and recording from the DA neurons resulted in a WT pattern of responding (Figure 3e, bottom).

DA neuron transmits positive and negative motivational value

Midbrain DAergic neuron activity is associated with reward-related behaviors and positive motivation.[38] Recent studies suggest that they also transmit signals related to aversive and alerting events.[39] We investigated the behavioral effect of selective DA cell excitation or inhibition by nicotine using an ICSA model based on choice behavior in a Y-maze[20–23] (Figure 4a). In this paradigm, WT mice actively self-administer nicotine at the dose of 100 ng per injection (Figure 4b), whereas $\beta2^{-/-}$ mice do not acquire this behavior.[24,27]

Here, we report that $\beta2^{DA-VEC}$ mice exhibited no acquisition of nicotine ICSA over the course of daily sessions, as evidenced by both the number of injections and latency (Figures 4c and d**)**. However, $\beta2^{DA-VEC}$ mice behaved differently from GFP-vectorized subjects: they exhibited initially a transient approach behavior toward the nicotine-reinforced arm, but did not develop a stable, chronic nicotine self-administration over sessions (Supplementary Figures S5a and b). In contrast, $\beta2^{GABA-VEC}$ exhibited a *decreased* choice of the reinforced arm, which remained below chance level (Figure 4c). Preferential choice of the non-reinforced arm is typically associated with the aversive effects of drugs of abuse, as previously demonstrated with cocaine.[23] To determine whether decreasing the nicotine dose would extend ICSA responding, the $\beta2^{DA-VEC}$ mice were tested further with lower concentrations of nicotine (see Supplementary Figures S5c and d). The use of a 50 ng dose led to an initial increase quickly followed by chance level responding, whereas no response was observed with the 10 ng dose. These results demonstrate that the β2 subunit expressed selectively on DA or GABA neurons of the VTA encodes, respectively, for positive or negative motivational value: direct excitation of DA neurons enhances the incentive value of nicotine, while inhibition of DA neurons through GABAergic excitation and/or direct inhibition of GABAergic efferent decreases it. However, in both cases nicotine effects were transient, as neither the positive (in $\beta2^{DA-VEC}$ mice) nor negative value (in $\beta2^{GABA-VEC}$ mice) were followed by subsequent acquisition of steady, chronic ICSA or avoidance.

A critical role for nicotine-evoked DA burst firing

To identify the mechanisms underlying stable ICSA acquisition, we studied DA release in response to nicotine and subsequent downstream signaling in DAergic target areas. *In vivo* microdialysis in freely moving mice was carried out to measure DA release after systemic injection of nicotine. Unlike WT mice, but similar to KO animals, the DA vectorized group did not exhibit a nicotine elicited increase in free DA (Figure 5a and Supplementary Figure S6). We then assessed the impact of this lack of DA release on DA-dependent cellular modifications in the NAc. The mitogen-activated protein kinase/ERK signaling pathway is activated by most drugs of abuse, including nicotine, within neurons of the NAc.[40] Interestingly, ERK activation caused by nicotine in the NAc critically depends on DA D1 receptor activation, as it is blocked by SCH23390, a D1 receptor antagonist. Furthermore, the blockade of ERK phosphorylation prevents immediate-early gene expression

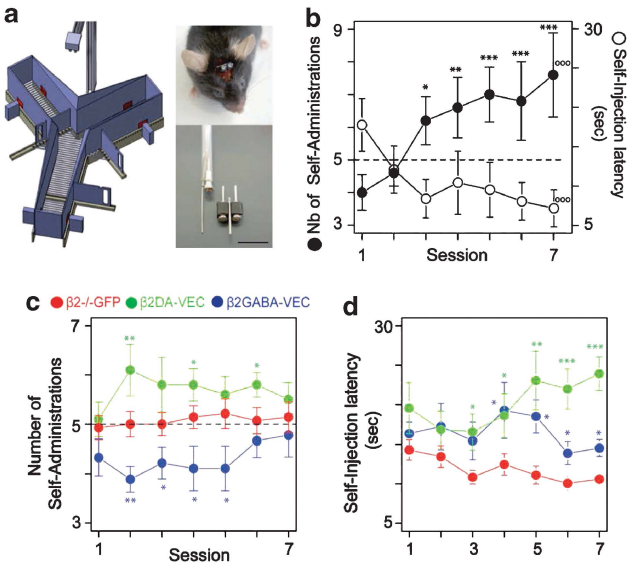

Figure 4. β2 Subunit re-expressed either on dopaminergic (DAergic) or γ-aminobutyric acid-releasing (GABAergic) neurons of the ventral tegmental area (VTA) encodes, respectively, for positive or negative motivational value. (**a**) The mouse model of intracranial nicotine self-administration (ICSA). (Left) Detailed three-dimensional sketch of the Y-maze apparatus used to assess choice of the nicotine-reinforced vs non-reinforced arm. (Right, top) Example of mouse implanted with the injection guide. (Right, bottom) Micro-connector, guide cannula and cannula used for intracranial injection of nicotine. Scale bar, 5 mm. (**b** Intra-VTA nicotine self-administration in wild-type (WT) (*$P<0.05$; **$P<0.01$; ***$P<0.001$; WT vs $\beta2^{GFP-VEC}$ (red; **c**). On the abscissa, the daily test sessions from days 1 to 7. On the left ordinate, the number of self-administration events per 10 daily trials, corresponding to the filled circles. On the right ordinate, self-injection latency in seconds. °°°$P<0.001$, session effect. (**c**) Intra-VTA nicotine self-administration in vectorized mice. Number of self-administrations in $\beta2^{DA-VEC}$ (green), $\beta2^{-/-}$ (red) and $\beta2^{GABA-VEC}$ (blue) mice per daily session (abscissa, 1–7) expressed as mean ± s.e.m., with 100 ng nicotine (as salt) per self-administered dose (*$P<0.05$; **$P<0.01$; ***$P<0.001$; $\beta2^{DA-VEC}$ or $\beta2^{GABA-VEC}$ vs $\beta2^{-/-}$; two-way analysis of variance (ANOVA); genotype effect: $F(2,30)=6.292$, $P<0.01$; session effect: $F(6,180)=0.793$, NS). (**d**) Self-injection latency in $\beta2^{DA-VEC}$ (blue), $\beta2^{-/-}$ (green) and $\beta2^{GABA-VEC}$ (red) mice. Ordinate, self-injection latency in seconds per daily session (abscissa, days 1–7) is expressed as mean ± s.e.m., with 100 ng nicotine (as salt) per self-administered dose (*$P<0.05$; **$P<0.01$; ***$P<0.001$; $\beta2^{DA-VEC}$ or $\beta2^{GABA-VEC}$ vs $\beta2^{-/-}$). VEC, vectorized.

and long-lasting behavioral changes associated with exposure to drugs of abuse.[41] Quantifying the number of phospho-ERK-positive nuclei in NAc revealed an abolition of ERK phosphorylation in response to nicotine in $\beta2^{-/-}$ mice (Figure 5b). This indicates a critical role of β2*-nAChRs in nicotine-elicited ERK activation in the NAc. It is of interest that we failed to restore ERK activation caused by nicotine in $\beta2^{DA-VEC}$ (Figure 5b). Therefore, nicotine elicited firing rate increase in $\beta2^{DA-VEC}$ is not sufficient to elicit DA release within the NAc, nor to activate downstream signaling pathways and maintain ICSA.

We then investigated the causes of transient ICSA. Because they have distinct influences on learning and motivation, tonic to phasic activity transitions are an essential component of the DA reward response.[42,43] Indeed, bursts are more effective in enhancing transmitter release,[44] and activating immediate-early genes in DA target areas.[45] Optogenetic methods have recently shown that the burst firing of DA neurons is a crucial property for reward.[46] We have therefore analyzed the burst structures in all of our groups by calculating the percentage of spikes within a burst (%SWB = number of spikes within burst divided by total number

of spikes in a 30 s time window, see Supplementary Material for details). Our previous work had shown that lentiviral re-expression of high-affinity nAChRs in the VTA using a ubiquitous PGK promoter results in nicotine-elicited burst firing.[15] However, burst analysis in $\beta2^{DA-VEC}$ and $\beta2^{GABA-VEC}$ mice revealed that acute systemic nicotine did not evoke bursting (Figure 5c). Only WT and $\beta2^{DA+GABA-VEC}$ mice, vectorized specifically in DA and GABA neurons of the VTA, exhibited a significant increase in burst firing. The analysis of spontaneous, acetylcholine-dependent activity is shown for firing rate in Figure 5d. This analysis is carried out as described in our previous publication.[15] For each neuron, spontaneous activity was quantified using firing rate (mean number of spikes per second) in Hz (Figure 5d, left) and %SWB (Figure 5d, right). These values are defined on the basis of at least 5 min of spontaneous activity before nicotine injection. It confirmed the role of GABA neurons in burst generation. In $\beta2^{GABA-VEC}$ and $\beta2^{DA+GABA-VEC}$ mice the spontaneous bursting pattern observed in the WT were restored, which was not the case in $\beta2^{DA-VEC}$. These results reveal that burst firing is a cooperative effect resulting from the interplay between direct excitation and inhibition.

We then tested a $\beta2^{DA+GABA-VEC}$ group in ICSA to determine whether habit-forming actions of nicotine could be observed in the doubly re-expressed mice. We found their nicotine-induced response to be strikingly similar to WT mice (Figure 5e). In contrast to $\beta2^{DA-VEC}$ mice, $\beta2^{DA+GABA-VEC}$ displayed a rapid and steady acquisition of nicotine ICSA. This means that burst firing can be correlated with stable ICSA acquisition.

DISCUSSION

One of the critical steps in the transition from nicotine intake to addiction is the development of nicotine-elicited habits that contribute to stimulate and maintain chronic consumption. Self-administration is a powerful behavioral paradigm to investigate important aspects of these critical early steps toward nicotine addiction.[47,48] Identifying, *in vivo*, the neural circuitry underlying the acquisition of nicotine self-administration provides essential clues to our understanding of nicotine addiction, and its treatment.

Novel lentiviral vectors for the cell-type-specific expression of nicotinic receptors

One of the major difficulties in analyzing the nicotinic system is that almost every neuron in the brain, and cells in most other tissues,[49] expresses nAChRs. We have therefore developed a general method for the neurotransmitter-specific expression of nAChRs through lentiviral vectors in the brain and applied it to the VTA of mice, the principal target of all drugs of abuse.[6,13] In the case of nicotine addiction, the cellular organization and relevant pharmacology of the VTA is complex as different nAChRs are present on a variety of cell types: DAergic projection neurons, local GABAergic neurons and terminals from cortical, pallidal and tegmental afferents (see Figure 1). Recently, also glutamatergic neurons have been identified in the VTA, but no data exist as to their expression of nicotinic receptors.[34,50] We have focused on the contribution of nAChRs on GABAergic neurons, which has been a challenging and little explored issue.[8,51] Our system allowed us to re-express exclusively the β2 nAChR subunit, responsible for high-affinity nAChRs, on either DAergic or GABAergic cells, or both in $\beta2^{DA+GABA-VEC}$ mice, in the VTA of β2 KOs. We demonstrate that the increase or decrease of DA firing frequency caused by nicotine acting exclusively on DA or GABA cells, respectively, correlates with positive or negative incentive value to drug-associated cues. However, only the concerted

Figure 5. Bursting activity and pharmacological consequences. (**a**) Microdialysis measuring extracellular dopamine (DA) levels in the nucleus accumbens (NAc) shell, showing area under the curve values (AUC, mean ± s.e.m. as % of baseline) during a 2 h post-treatment period. $^*P<0.05$ and NS = not statistically significant (wild-type (WT), black, $n=9$; $\beta2^{-/-}$, red, $n=6$; $\beta2^{DA-VEC}$, green, $n=7$ mice per group). Open bars, injection of saline. Filled-in bars, response to nicotine. (**b**) Quantification of increase in the number of phosphorylated-extracellular signal-regulated kinase (P-ERK)-positive nuclei after acute nicotine injection in mice. (Top) Photomicrographs of the NAc showing P-ERK immunostained neurons after saline (upper row) and nicotine (bottom row) administration. Arrowheads point to several P-ERK-positive nuclei. (Bottom) Quantification of increase in the number of P-ERK-positive nuclei after acute nicotine injection in WT mice (black, $n=4$ for saline and nicotine, $P<0.05$, Wilcoxon's signed-rank test), $\beta2^{-/-}$ mice (red, $n=3$ for saline and nicotine, $P>0.05$, exact Wilcoxon's signed-rank test), $\beta2^{DA-VEC}$ mice (green, $n=3$ for saline and nicotine, $P>0.05$, Wilcoxon's signed-rank test). (**c**) Nicotine-elicited modifications of the percent of spikes within bursts (%SWB) (mean ± s.e.m.) in VTA DAergic neurons of WT mice (black, $n=43$, mean of the maximal variation $+15.42\pm3.68\%$, $P=6.78\times10^{-6}$, paired Wilcoxon's test), $\beta2^{DA-VEC}$ (green, $n=20$, mean of the maximal variation $+0.97\pm1.03\%$, $P=0.724$, paired Wilcoxon's test), $\beta2^{GFP-VEC}$ ($n=27$, mean of the maximal variation $+0.27\pm0.69\%$, $P=0.16$, paired Wilcoxon's test), $\beta2^{GABA-VEC}$ (blue, $n=30$, mean of the maximal variation $-3.76\pm1.63\%$, $P=0.0025$, paired Wilcoxon's test) and $\beta2^{DA+GABA-VEC}$ mice (purple, $n=13$, mean of the maximal variation $+6.49\pm1.67\%$, $P=0.0028$, paired Wilcoxon's test). Vertical dashed line indicates the nicotine injection (blue). Horizontal dashed lines indicate the baseline level (red, for value see **d**). Group comparison: WT vs $ß2^{-/-}$, $P=0.005$; WT vs $\beta2^{DA-VEC}$, $P=0.005$; WT vs $\beta2^{GABA-VEC}$, $P=8.4\times10^{-7}$; $ß2^{-/-}$ vs $\beta2^{GABA-VEC}$, $P=3.7\times10^{-5}$; $\beta2^{-/-}$ vs $\beta2^{DA+GABA-VEC}$, $P=0.0005$ (Wilcoxon's signed rank test with a sequential Bonferroni correction, only significant comparisons are indicated, see Supplementary Material). (**d**) Quantification of spontaneous firing of DA cells. (Left) Bar-plot representation of the mean basal firing rate (Hz) represented as means ± s.e.m. WT (black, $n=43$, mean $=3.31\pm0.27$ Hz), $ß2^{-/-}$ (red, $n=27$, mean $=2.28\pm0.17$ Hz), $ß2^{DA-VEC}$ (green, $n=20$, mean $=2.62\pm0.24$ Hz), $ß2^{GABA-VEC}$ (blue, $n=30$, mean $=3.48\pm0.33$ Hz) and $\beta2^{DA+GABA-VEC}$ mice (purple, $n=30$, mean $=2.29\pm0.43$ Hz). Group comparison: WT vs $\beta2^{-/-}$, $P=0.006$; $\beta2^{-/-}$ vs $ß2^{GABA-VEC}$, $P=0.004$ (Wilcoxon's signed-rank test with a sequential Bonferroni correction, $^{**}P<0.01$; see Figure 3e and Supplementary Material for statistical procedures). (Right) Bar-plot representation of the %SWB represented as means ± s.e.m. WT (black, mean $=11.19\pm2.75\%$), $\beta2^{-/-}$ (red, $n=27$, mean $=1.38\pm0.64\%$), $\beta2^{DA-VEC}$ (green, $n=20$, mean $=1.74\pm1.13\%$), $\beta2^{GABA-VEC}$ (blue, $n=30$, mean $=15.08\pm5.09\%$) and $\beta2^{DA+GABA-VEC}$ mice (purple, $n=13$, mean $=9.37\pm5.38\%$). Group comparison: WT vs $\beta2^{-/-}$, $P=0.001$; WT vs $ß2^{DA-VEC}$, $P=0.0048$; $\beta2^{-/-}$ vs $ß2^{GABA-VEC}$, $P=0.0073$; $\beta2^{-/-}$ vs $ß2^{DA+GABA-VEC}$, $P=0.012$ (Wilcoxon's signed-rank test with a sequential Bonferroni correction, only significant comparisons are indicated; see Figure 3e and Supplementary Material for statistical procedures). (**e**) Number of self-administrations (circle, solid line) in $\beta2^{DA+GABA-VEC}$ (empty circle) and WT mice (full circle) per daily session (abscissa, 1–5) expressed as mean ± s.e.m., with 100 ng nicotine (as salt) per self-administered dose (two-way analysis of variance (ANOVA), genotype effect: $F(1,10)=2.357$, NS; session effect: $F(4,40)=17.136$, $P<0.001$; genotype × session effect: $F(4,40)=1.717$, NS. $^*P<0.05$; $^{**}P<0.01$; $^{***}P<0.001$ as compared to chance level). $\beta2^{DA+GABA-VEC}$ displayed a steady nicotine self-administration and earned significantly more self-injections than $\beta2^{DA-VEC}$ ($F1,14=7.738$, $P<0.02$) and $\beta2^{-/-}$ ($F1,12=16.331$, $P<0.01$). As typically observed during acquisition of intracranial self-administration (ICSA), the self-injection latency (triangle, dashed lines) decreased over sessions, this effect being similar in $\beta2^{DA+GABA-VEC}$ (empty triangle) and WT (full triangle) (genotype effect: $F1,10=0.126$, NS; Session effect: $F4,40=3.247$, $P<0.05$). $\beta2^{DA+GABA-VEC}$ also triggered nicotine injections faster than $\beta2^{DA-VEC}$ ($F1,14=8.735$, $P<0.01$) and tend to be even faster than $\beta2^{-/-}$, which are known to exhibit a spontaneously active phenotype ($F1,12=4.213$, $P<0.06$). VEC, vectorized.

activation of nAChRs on DAergic *and* GABAergic cells correlates with the acquisition of a steady nicotine self-administration.

A crucial role for burst firing of DAergic neurons in nicotine reinforcement

We show that a particular firing pattern of the DA neurons, burst firing, is a critical physiological mechanism required for the long-term acquisition of nicotine self-administration. Tonic to phasic transition is an essential part of the functional role of the DAergic system.[43] DA cell bursts of action potentials are related to elevated DA outflow and to the signaling of novel rewards or environmental stimuli.[43,52] Disruption of NMDA receptor-dependent burst firing impairs the acquisition of several conditioned behavioral responses and learning about cues that predict salient events.[53] In addition, optogenetic tools have been used recently to demonstrate that DA bursting activity is sufficient to mediate reinforcement.[46] Burst firing can be triggered by a number of events.[54,55] Among these are glutamatergic receptor activation,[53] activation of voltage-gated ion channels following NMDA receptor activation,[56] alteration of SK conductance[57,58] and decrease of tonic GABAergic inhibition. However, our results suggest that cholinergic input,

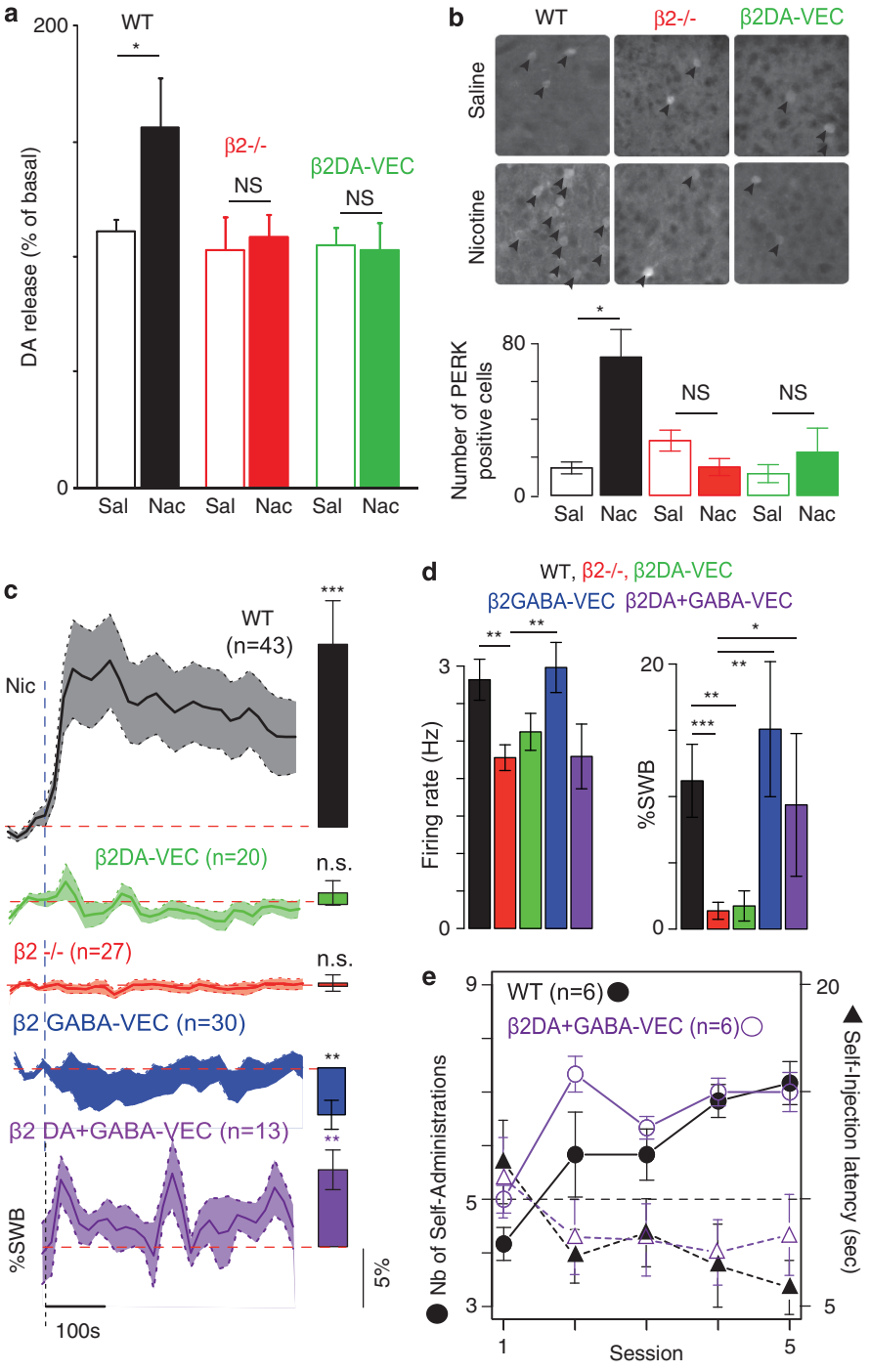

relying on the activation of α4α6β2*-nAChR expressed within the VTA,[15,27,29,30,59] play the role of a permissive gate that allows these various stimuli to trigger burst firing.[60–62]

In this paper we show, however, that β2*-nAChRs at the level of VTA DA cells alone are not sufficient to restore bursts evoked by nicotine. Accordingly, as a functional readout, we failed to restore ERK activation induced in the NAc by nicotine in $\beta2^{DA-VEC}$ mice and an increase in DA release. These data suggest, first, that an increase in frequency due to β2*-nAChRs on DA cells can be dissociated from enhancement of bursting, and second, that cholinergic input from tegmental nuclei also has a key role on GABA cells, and on burst control.

Redefining the role for VTA GABA neurons

The role we assign to GABAergic interneurons in the VTA differs significantly from proposals formulated over the past decade on the basis of data obtained with *in vitro* slice preparations.[9,11,12] Although Mansvelder and McGehee[9] did show some transient activation of GABAergic neurons in slices, all subsequent models describing the acute effect of nicotine on DA cell excitability were centered on disinhibition following GABA cell desensitization, and glutamatergic activation. Our results emphasize the role of ß2*-nAChRs on DA cells to increase firing, and importantly, on the interplay between DA and GABA activation to produce burst firing, the key property of DA neurons. An increase in GABAergic activity, and not a decrease, is thus necessary to shape DA cell bursting.

Our initial results on GABA neuron activation (Figure 2b) might be seen difficult to interpret directly as a GABA-mediated inhibition for two reasons. First, in these experiments we recorded 'putative' GABAergic neurons. Second, GABAergic neurons in the VTA are not exclusively interneurons as some of them project to the same forebrain targets as do the DA neurons.[63] Nicotine-dependent excitation could thus be an exclusive property of GABAergic neurons that project outside the VTA. To circumvent conclusively these issues, we focused our electrophysiological analyses on DA cells, and on the effect of ß2*-nAChR activation on GABAergic interneurons using cell-type-specific expression of nicotinic receptors (Figure 3). Our results demonstrate that these GABAergic *inter*neurons are activated by nicotine, and consequently inhibit DA cell firing (see Figure 3e). This major novel finding is substantiated by unambiguous identification and labeling of the recorded DA neurons (see Figure 3d and Supplementary Information). Interestingly, the minimal computational model with nAChRs expressed only on the DA cells also reproduces the shorter time courses of the DA response in $\beta2^{DA-VEC}$ animals as compared to the WT (compare green and grey lines in Figure 2e). And in the models with GABA-nAChRs, an increase above baseline after inhibition is observed in $\beta2^{GABA-VEC}$ (compare Figure 2e to Figure 2f). This further supports the notion that late, but not short-term, DA responses are governed by receptor desensitization.

We also show that cholinergic modulation of GABAergic cells is required for spontaneous DA neuron bursting. Recent data suggest that GABAergic input can act through phasic disinhibition as an excitatory drive, promoting rebound burst firing in DA neurons.[64,65] In line with this view, our results demonstrate conclusively that re-expression of the β2 subunit in GABA neurons allows spontaneous burst firing in DA neurons. In $\beta2^{GABA-VEC}$ mice, increased GABAergic input causes increased IPSPs in DA neurons, which has been shown to produce irregular firing patterns,[66] allowing us to link the restoration of spontaneous bursting in DA neurons with the cholinergic modulation of GABA neuron activity.

Finally, burst firing and irregularity would require a balance between excitation and inhibition. Strong and synchronous activation of GABAergic cells, such as those caused by nicotine in $\beta2^{GABA-VEC}$ DA neurons, cannot evoke bursting in DA cells if it is not counterbalanced by excitation. We suggest that this balance is endorsed by β2*-nAChRs expressed, respectively, at the DA and GABA level within the VTA as suggested by our results on $\beta2^{DA+GABA-VEC}$ mice.

Towards a comprehensive understanding of the *in vivo* effects of nicotine

There are a number of conundrums in the study of the *in vivo* effects of nicotine: we show that, in mice, nicotine modulates the nAChRs in a few seconds, activation of DA neurons persists for about 10 min, and nicotine-dependent axonal release of DA lasts for 1–2 h. Finally, behavioral effects such as those observed in self-administration protocols take several days to be established. We have started to tackle the mechanisms of these different timescales and their significance. In particular, our computational modeling shows that a rapid phasic increase of DA activity, and hence a DA output spike, is likely to be due to the direct excitation of receptors on DA neurons, whereas the longer lasting increase of DA firing rate by nicotine is due to desensitization of GABA neuron nAChRs. The latter may also be a mechanism that shifts the DA cell activity from tonic to bursting.[67] Further computational study has suggested that receptor desensitization by nicotine may play an important role in shaping DA responses to environmental stimuli, notably reducing the impact of negative motivational stimuli and rendering DA responding to previously learned stimuli again labile.[68]

It is generally admitted that tobacco and nicotine are repeatedly used because they provide positive feelings, and that this is linked with the increased activity in the mesocorticolimbic DA system.[69] There is some initial evidence that VTA DAergic cells encode rewarding and aversive stimuli by increases and decreases of their firing frequency, respectively.[39] We show here with our experiments using $\beta2^{DA-VEC}$ and $\beta2^{GABA-VEC}$ mice that this increase in DA firing frequency caused by nicotine correlates with a positive or negative incentive value to stimuli, whereas decreased DA firing frequency and increased VTA GABA neuron activity correlates with a negative incentive value. Indeed, we cannot exclude that VTA GABA neurons may alter reward function not only by their interaction with DA neurons and their burst patterns, but also with their interaction with the downstream targets in the mesolimbic and mesocortical DA terminal fields, or the tegmentum.[10] However, this result suggests that nicotine can transmit positive and negative value as a function of its action on DAergic or GABAergic neurons in the VTA. A number of different drugs, and in particular nicotine, have been postulated to act through disinhibition of the DA system.[14] According to this view, the GABAergic system acts to support and enhance excitatory input to DA neurons via somatic or presynaptic activation. Our results rather suggest that, while a predominant influence of GABA would elicit mainly aversive effects,[10] the co-activation of DA and GABA systems is required for the habit-forming action of nicotine.[70]

A novel mechanism, potentially defining a novel drug target

We elucidate, for the first time, microcircuits engaged *in vivo* in a critical step of drug addiction and its regulation by endogenous neurotransmitters. We propose that within the VTA, DA-GABA neuron interplay is essential for the acquisition of persistent nicotine-directed behavior. Now, we need to further establish the role of GABAergic neurons in the chronic response to nicotine. Future studies should investigate how GABAergic activity is required for the long-term maintenance of nicotine dependence and the relevant loss of control, thus identifying a potentially novel drug target. Chronic nicotine exposure upregulates specifically the amount of nAChRs containing the α4 subunit in GABAergic neurons.[51] Our study thus could pave the way for the development and pre-clinical testing of smoking cessation agents, targeting the heteromeric α4β2-containing receptors on

GABAergic interneurons, and *not* DAergic receptors, as frequently attempted by pharmaceutical companies.[3]

CONFLICT OF INTEREST

The authors declare no conflict of interest.

ACKNOWLEDGEMENTS

We thank Benoît Forget and Henri Korn for helpful comments on the manuscript, and Jochen Roeper for help with slice electrophysiology. This work was supported by the Institut Pasteur, Centre National de la Recherche Scientifique CNRS URA 2182, UMR 7102, UMR 5287 and ATIP programme, the Agence Nationale pour la Recherche (ANR Neuroscience, Neurologie et Psychiatrie 2005 and 2009, and ANR BLANC 2009), Neuropôle IdF, INSERM U960, the RTRA Ecole des Neurosciences de Paris and the Bettencourt Schueller Foundation. The research leading to these results has received funding from the European Union Seventh Framework Programme under Grant no. HEALTH-F2-2008-202088 ('NeuroCypres' project to U.M.). ST acknowledges financial support from Fondation de la Recherche Médicale (FRM), and Pasteur-Weizmann.

REFERENCES

1 WHO. World Health Organization Report on the Global Tobacco Epidemic, available from: http://www.who.int/tobacco/mpower/2009/en/, 2009.
2 Changeux JP. Nicotine addiction and nicotinic receptors: lessons from genetically modified mice. *Nat Rev Neurosci* 2010; **11**: 389–401.
3 Taly A, Corringer PJ, Guedin D, Lestage P, Changeux JP. Nicotinic receptors: allosteric transitions and therapeutic targets in the nervous system. *Nat Rev Drug Discov* 2009; **8**: 733–750.
4 Marti F, Arib O, Morel C, Dufresne V, Maskos U, Corringer PJ *et al.* Smoke extracts and nicotine, but not tobacco extracts, potentiate firing and burst activity of ventral tegmental area dopaminergic neurons in mice. *Neuropsychopharmacology* 2011; **36**: 2244–2257.
5 Changeux JP, Edelstein SJ. *Nicotinic Acetylcholine Receptors: From Molecular Biology to Cognition*. Odile Jacob: New York, 2005.
6 Pontieri FE, Tanda G, Orzi F, Chiara GD. Effects of nicotine on the nucleus accumbens and similarity to those of addictive drugs. *Nature* 1996; **382**: 255–257.
7 Picciotto MR, Zoli M, Rimondini R, Lena C, Marubio LM, Pich EM *et al.* Acetylcholine receptors containing the beta2 subunit are involved in the reinforcing properties of nicotine. *Nature* 1998; **391**: 173–177.
8 Klink R, de Kerchove d'Exaerde A, Zoli M, Changeux JP. Molecular and physiological diversity of nicotinic acetylcholine receptors in the midbrain dopaminergic nuclei. *J Neurosci* 2001; **21**: 1452–1463.
9 Mansvelder HD, McGehee DS. Cellular and synaptic mechanisms of nicotine addiction. *J Neurobiol* 2002; **53**: 606–617.
10 Laviolette SR, van der Kooy D. The neurobiology of nicotine addiction: bridging the gap from molecules to behaviour. *Nat Rev Neurosci* 2004; **5**: 55–65.
11 Mansvelder HD, Keath JR, McGehee DS. Synaptic mechanisms underlie nicotine-induced excitability of brain reward areas. *Neuron* 2002; **33**: 905–919.
12 Mansvelder HD, McGehee DS. Long-term potentiation of excitatory inputs to brain reward areas by nicotine. *Neuron* 2000; **27**: 349–357.
13 Luscher C, Malenka RC. Drug-evoked synaptic plasticity in addiction: from molecular changes to circuit remodeling. *Neuron* 2011; **69**: 650–663.
14 Sulzer D. How addictive drugs disrupt presynaptic dopamine neurotransmission. *Neuron* 2011; **69**: 628–649.
15 Mameli-Engvall M, Evrard A, Pons S, Maskos U, Svensson TH, Changeux JP *et al.* Hierarchical control of dopamine neuron-firing patterns by nicotinic receptors. *Neuron* 2006; **50**: 911–921.
16 Dani JA, Bertrand D. Nicotinic acetylcholine receptors and nicotinic cholinergic mechanisms of the central nervous system. *Annu Rev Pharmacol Toxicol* 2007; **47**: 699–729.
17 Olivo-Marin JC. Extraction of spots in biological images using multiscale products. *Pattern Recogn* 2002; **35**: 1989–1996.
18 Tolu S, Avale ME, Nakatani H, Pons S, Parnaudeau S, Tronche F *et al.* A versatile system for the neuronal subtype specific expression of lentiviral vectors. *FASEB J* 2010; **24**: 723–730.
19 Maskos U, Molles BE, Pons S, Besson M, Guiard BP, Guilloux JP *et al.* Nicotine reinforcement and cognition restored by targeted expression of nicotinic receptors. *Nature* 2005; **436**: 103–107.
20 David V, Cazala P. A comparative study of self-administration of morphine into the amygdala and the ventral tegmental area in mice. *Behav Brain Res* 1994; **65**: 205–211.
21 David V, Durkin TP, Cazala P. Differential effects of the dopamine D2/D3 receptor antagonist sulpiride on self-administration of morphine into the ventral tegmental area or the nucleus accumbens. *Psychopharmacology (Berl)* 2002; **160**: 307–317.
22 David V, Segu L, Buhot MC, Ichaye M, Cazala P. Rewarding effects elicited by cocaine microinjections into the ventral tegmental area of C57BL/6 mice: involvement of dopamine D1 and serotonin1B receptors. *Psychopharmacology (Berl)* 2004; **174**: 367–375.
23 David V, Gold LH, Koob GF, Cazala P. Anxiogenic-like effects limit rewarding effects of cocaine in balb/cbyj mice. *Neuropsychopharmacology* 2001; **24**: 300–318.
24 David V, Besson M, Changeux JP, Granon S, Cazala P. Reinforcing effects of nicotine microinjections into the ventral tegmental area of mice: dependence on cholinergic nicotinic and dopaminergic D1 receptors. *Neuropharmacology* 2006; **50**: 1030–1040.
25 Mason PA, Milner PM, Miousse R. Preference paradigm: provides better self-stimulation reward discrimination than a rate-dependent paradigm. *Behav Neural Biol* 1985; **44**: 521–529.
26 David V, Matifas A, Gavello-Baudy S, Decorte L, Kieffer BL, Cazala P. Brain regional Fos expression elicited by the activation of mu- but not delta-opioid receptors of the ventral tegmental area: evidence for an implication of the ventral thalamus in opiate reward. *Neuropsychopharmacology* 2008; **33**: 1746–1759.
27 Maskos U. Emerging concepts: novel integration of *in vivo* approaches to *localise* the function of nicotinic receptors. *J Neurochem* 2007; **100**: 596–602.
28 Wise R. Brain reward circuitry: insights from unsensed incentives. *Neuron* 2002; **36**: 229–240.
29 Maskos U. The cholinergic mesopontine tegmentum is a relatively neglected nicotinic master modulator of the dopaminergic system: relevance to drugs of abuse and pathology. *Br J Pharmacol* 2008; **153**(Suppl 1): S438–S445.
30 Maskos U. Role of endogenous acetylcholine in the control of the dopaminergic system via nicotinic receptors. *J Neurochem* 2010; **114**: 641–646.
31 Petersen DR, Norris KJ, Thompson JA. A comparative study of the disposition of nicotine and its metabolites in three inbred strains of mice. *Drug Metab Dispos* 1984; **12**: 725–731.
32 Graupner M, Gutkin BS. Modeling nicotinic neuromodulation from global functional and network levels to nAChR based mechanisms. *Acta Pharmacol Sin* 2009; **30**: 681–693.
33 Graupner M, Gutkin BS In: Gutkin BS, Ahmed SH (eds). *Computational Neuroscience of Drug Addiction, Computational Neuroscience Series*. Springer Verlag: Berlin, 2011, pp 111–144.
34 Dobi A, Margolis EB, Wang H-L, Harvey BK, Morales M. Glutamatergic and nonglutamatergic neurons of the ventral tegmental area establish local synaptic contacts with dopaminergic and nondopaminergic neurons. *J Neurosci* 2010; **30**: 218–229.
35 Graupner M, Gutkin BS. Tonic acetylcholine governs the phasic mesolimbic dopamine response to nicotine. *PLoS Comp Biol* 2012 (under consideration).
36 Turiault M, Parnaudeau S, Milet A, Parlato R, Rouzeau JD, Lazar M *et al.* Analysis of dopamine transporter gene expression pattern—generation of DAT-iCre transgenic mice. *FEBS J* 2007; **274**: 3568–3577.
37 Fuchs EC, Doheny H, Faulkner H, Caputi A, Traub RD, Bibbig A *et al.* Genetically altered AMPA-type glutamate receptor kinetics in interneurons disrupt long-range synchrony of gamma oscillation. *Proc Natl Acad Sci USA* 2001; **98**: 3571–3576.
38 Fields HL, Hjelmstad GO, Margolis EB, Nicola SM. Ventral tegmental area neurons in learned appetitive behavior and positive reinforcement. *Annu Rev Neurosci* 2007; **30**: 289–316.
39 Bromberg-Martin ES, Matsumoto M, Hikosaka O. Dopamine in motivational control: rewarding, aversive, and alerting. *Neuron* 2010; **68**: 815–834.
40 Valjent E, Pages C, Herve D, Girault JA, Caboche J. Addictive and non-addictive drugs induce distinct and specific patterns of ERK activation in mouse brain. *Eur J Neurosci* 2004; **19**: 1826–1836.
41 Girault JA, Valjent E, Caboche J, Herve D. ERK2: a logical AND gate critical for drug-induced plasticity? *Curr Opin Pharmacol* 2007; **7**: 77–85.
42 Grace AA. Phasic versus tonic dopamine release and the modulation of dopamine system responsivity: a hypothesis for the etiology of schizophrenia. *Neuroscience* 1991; **41**: 1–24.
43 Schultz W. Multiple dopamine functions at different time courses. *Annu Rev Neurosci* 2007; **30**: 259–288.
44 Gonon FG. Nonlinear relationship between impulse flow and dopamine released by rat midbrain dopaminergic neurons as studied by *in vivo* electrochemistry. *Neuroscience* 1988; **24**: 19–28.
45 Chergui K, Svenningsson P, Nomikos GG, Gonon F, Fredholm BB, Svennson TH. Increased expression of NGFI-A mRNA in the rat striatum following burst stimulation of the medial forebrain bundle. *Eur J Neurosci* 1997; **9**: 2370–2382.
46 Tsai HC, Zhang F, Adamantidis A, Stuber GD, Bonci A, de Lecea L *et al.* Phasic firing in dopaminergic neurons is sufficient for behavioral conditioning. *Science* 2009; **324**: 1080–1084.
47 Corrigall WA. Nicotine self-administration in animals as a dependence model. *Nicotine Tob Res* 1999; **1**: 11–20.

48 Rose JE, Corrigall WA. Nicotine self-administration in animals and humans: similarities and differences. *Psychopharmacology (Berl)* 1997; **130**: 28–40.
49 Wessler I, Kirkpatrick CJ. Acetylcholine beyond neurons: the non-neuronal cholinergic system in humans. *Br J Pharmacol* 2008; **154**: 1558–1571.
50 Nair-Roberts RG, Chatelain-Badie SD, Benson E, White-Cooper H, Bolam JP, Ungless MA. Stereological estimates of dopaminergic, GABAergic and glutamatergic neurons in the ventral tegmental area, substantia nigra and retrorubral field in the rat. *Neuroscience* 2008; **152**: 1024–1031.
51 Nashmi R, Xiao C, Deshpande P, McKinney S, Grady SR, Whiteaker P *et al.* Chronic nicotine cell specifically upregulates functional alpha 4* nicotinic receptors: basis for both tolerance in midbrain and enhanced long-term potentiation in perforant path. *J Neurosci* 2007; **27**: 8202–8218.
52 Schultz W. Getting formal with dopamine and reward. *Neuron* 2002; **36**: 241–263.
53 Zweifel LS, Parker JG, Lobb CJ, Rainwater A, Wall VZ, Fadok JP *et al.* Disruption of NMDAR-dependent burst firing by dopamine neurons provides selective assessment of phasic dopamine-dependent behavior. *Proc Natl Acad Sci USA* 2009; **106**: 7281–7288.
54 Overton PG, Clark D. Burst firing in midbrain dopaminergic neurons. *Brain Res* 1997; **25**: 312–334.
55 Tepper JM, Lee CR In: Tepper JM, Abercrombie ED, Bolam JP (eds). *Progress in Brain Research* **Vol. 160**. Elsevier: Amsterdam, 2007, pp189–208.
56 Deister CA, Teagarden MA, Wilson CJ, Paladini CA. An intrinsic neuronal oscillator underlies dopaminergic neuron bursting. *J Neurosci* 2009; **29**: 15888–15897.
57 Canavier CC, Landry RS. An increase in AMPA and a decrease in SK conductance increase burst firing by different mechanisms in a model of a dopamine neuron *in vivo*. *J Neurophysiol* 2006; **96**: 2549–2563.
58 Kitai ST, Shepard PD, Callaway JC, Scroggs R. Afferent modulation of dopamine neuron firing patterns. *Curr Opin Neurobiol* 1999; **9**: 690–697.
59 Exley R, Maubourguet N, David V, Eddine R, Evrard A, Pons S *et al.* Distinct contributions of nicotinic acetylcholine receptor subunit {alpha}4 and subunit {alpha}6 to the reinforcing effects of nicotine. *Proc Natl Acad Sci USA* 2011; **108**: 7577–7582.
60 Floresco SB, West AR, Ash B, Moore H, Grace AA. Afferent modulation of dopamine neuron firing differentially regulates tonic and phasic dopamine transmission. *Nat Neurosci* 2003; **6**: 968–973.
61 Grace AA, Floresco SB, Goto Y, Lodge DJ. Regulation of firing of dopaminergic neurons and control of goal-directed behaviors. *Trends Neurosci* 2007; **30**: 220–227.
62 Lodge DJ, Grace AA. The laterodorsal tegmentum is essential for burst firing of ventral tegmental area dopamine neurons. *Proc Natl Acad Sci USA* 2006; **103**: 5167–5172.
63 Omelchenko N, Sesack SR. Ultrastructural analysis of local collaterals of rat ventral tegmental area neurons: GABA phenotype and synapses onto dopamine and GABA cells. *Synapse* 2009; **63**: 895–906.
64 Hong S, Hikosaka O. The globus pallidus sends reward-related signals to the lateral habenula. *Neuron* 2008; **60**: 720–729.
65 Lobb CJ, Wilson CJ, Paladini CA. A dynamic role for GABA receptors on the firing pattern of midbrain dopaminergic neurons. *J Neurophysiol* 2010; **104**: 403–413.
66 Grace AA, Bunney BS. Opposing effects of striatonigral feedback pathways on midbrain dopamine cell activity. *Brain Res* 1985; **333**: 271–284.
67 Oster MA, Faure P, Gutkin BS. *Society for Neuroscience Annual Meeting*. San Diego, CA, 2010.
68 Graupner M, Gutkin BS. *Society for Neuroscience Annual Meeting*. Chicago, IL, 2009.
69 Miwa JM, Freedman R, Lester HA. Neural systems governed by nicotinic acetylcholine receptors: emerging hypotheses. *Neuron* 2011; **70**: 20–33.
70 Dalley JW, Everitt BJ, Robbins TW. Impulsivity, compulsivity, and top–down cognitive control. *Neuron* 2011; **69**: 680–694.

Supplementary Information accompanies the paper on the Molecular Psychiatry website (http://www.nature.com/mp)